Available online at www.sciencedirect.com

ScienceDirect

Journal of the European Ceramic Society 34 (2014) 3699–3706

www.elsevier.com/locate/jeurceramsoc

Electric field-assisted sintering of tin dioxide with manganese dioxide addition

E.N.S. Muccillo *, R. Muccillo *

Center of Science and Technology of Materials Energy and Nuclear Research Institute Trav. R 400, Cidade Universitária, São Paulo, SP, Brazil

Received 7 March 2014; received in revised form 8 May 2014; accepted 22 May 2014
Available online 13 June 2014

Abstract

Green compacts of pure SnO_2 and with addition of 0.25, 0.5 and 1.0 wt.% MnO_2 were sintered by applying 100 V cm^{-1} at 1 kHz and limiting the current to 5 A during 5 min at 1100 and 1200 °C. The shrinkage was monitored precisely during the electric current pulses. The role played by the additive was clearly seen in the shrinkage data: the higher is the additive content the lower is the onset of the shrinkage and the higher is the attained final shrinkage level. Sintering experiments on cylindrical samples with 0.5 wt.% MnO_2 with different thickness-to-diameter ratio show that the lower is that ratio, the higher is the shrinkage level, showing that the imparted Joule heating play a key role in the mechanisms responsible for sintering. The total electrical resistivity, evaluated by impedance spectroscopy, depends on the maximum attained shrinkage level, due to pore elimination upon sintering.
© 2014 Elsevier Ltd. All rights reserved.

Keywords: Electric field-assisted sintering; Tin dioxide; Impedance spectroscopy

1. Introduction

The importance of SnO_2 semiconductor ceramics is reflected by the wide range of application of this material, described in reviews on monolithic ceramics[1] as well as on hierarchical nanostructures.[2]

Tin dioxide (SnO_2), a semiconductor known to be difficult to sinter, was recently reported by the authors to be successfully sintered at 1100 °C when exposed to electric current pulses resulting from the application of ac electric fields.[3] Pure SnO_2 powder compacts do not get dense by conventional sintering because there is the predominance of an evaporation-condensation mechanism due to its high vapor pressure value.[4–6]

Manganese dioxide is reported to have very low solubility in tin dioxide; upon mixing and heating, the manganese cation is positioned in a very thin segregation layer surrounding the tin dioxide grains.[7] The sintering of tin dioxide with addition of manganese dioxide (melting point ~535 °C) was reported to create oxide ion vacancies at the grain interfaces and therefore to promote densification via vacancy-assisted grain boundary diffusion.[7–9]

Electric field-assisted sintering of SnO_2,[3] SiC[10] and TiO_2[11] semiconductors have already been reported. The common interest in those papers is the ability of that sintering technique to obtain sintered polycrystalline ceramic bodies either saving energy (lower sintering temperature, short sintering times) or attaining desirable microstructure features not easily reached by conventional approaches. Particle–particle contact promoted by Joule heating was considered the main reason for enhanced sintering of SiC.[10] Moreover, additives were found to be important for obtaining near full density SiC. Similar to the behavior of electric field-assisted sintered SnO_2,[3] bulky SiC specimens sinter better at the center than at the border. This could be due either to heterogeneous green microstructure or to the very fast sintering time (order of seconds, not enough to transfer heat through the whole sample). This problem could be circumvented by stacking the specimen between a material with low (thermal) conductivity. This density gradient is not reported by others[11–18], probably because their experiments were performed with relatively thinner specimens.

* Corresponding authors. Tel.: +55 11 31339203; fax: +55 11 31339276.
E-mail addresses: enavarro@usp.br (E.N.S. Muccillo), muccillo@usp.br (R. Muccillo).

http://dx.doi.org/10.1016/j.jeurceramsoc.2014.05.035
0955-2219/© 2014 Elsevier Ltd. All rights reserved.

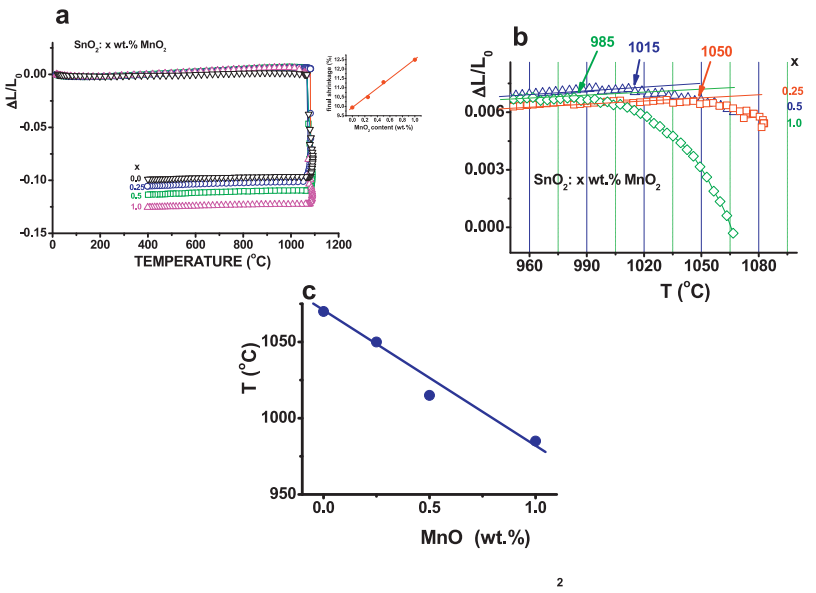

Fig. 1. (a) Dilatometric curves of ϕ 5 mm × 5.3 mm thickness SnO_2:x wt.% MnO_2, x = 0, 0.25, 0.5 and 1.0, green compacts upon heating to 1100 °C and application of 110 V cm^{-1}. Inset: final shrinkage dependence on MnO_2 content; (b) detail of increasing temperature data of (a); (c) onset temperature for shrinkage as a function of MnO_2 content.

In our previous paper we investigated two effects on the final densification of pure and SnO_2 + 2.0 wt.% MnO_2.[3] One is the limitation of the electric current through the sample under an ac electric field. This limitation is important to avoid a thermal runaway with a continuous increase in the electric current, which could even provoke the melting of the sample. The limit value to be chosen depends on the electrical behavior of the sample at the temperature the electric voltage is applied. The other effect is the use of manganese dioxide as a sintering aid. Briefly, it was shown that increasing the limit current from 1 A to 5 A, a shrinkage level of 20% is achieved, whereas without the sintering aid, the grains are welded together without significant densification.

Suitable processing procedures have to be taken into account for a successful sintering. Conventional sintering requires the knowledge of powder size, firing time, temperature, additives and atmosphere.[19] In the electric field-assisted sintering one has to consider further the electrical behavior of the specimen as a function of temperature.

Here, we evaluate the effect of the sintering aid content on the linear shrinkage level. Moreover, for a fixed amount of sintering aid (0.5 wt.% MnO_2) the influence of the sample dimensions (volume effect), important for the scale up of the electric field-assisted technique to actual ceramic pieces, was also investigated.

2. Experimental

SnO_2 obtained by calcination in air at 900 °C of SnO and MnO_2 (both Alfa Aesar 99.9%) were dried, weighed, mixed thoroughly in an agate mortar, and pressed (ϕ 5 mm to 3–5 mm thick disks) in stoichiometry contents to produce SnO_2:x wt.% MnO_2, x = 0, 0.25, 0.5 and 1.0 green compacts. Samples with 0.5 wt.% MnO_2 were prepared with different thicknesses to evaluate the effect of the thickness-to-diameter ratio on the final shrinkage under similar imparted electric field. The X-ray fluorescence analysis of electric field-assisted sintered pellets, performed in a Shimadzu EDX-720 equipment, showed that the manganese content is nearly the same as the nominal addition. The electric field-assisted sintering experiment was conducted in a laboratory setup described in detail elsewhere.[3,20] The sintering process occurs inside a dilatometer, which allows to monitor shrinkage while applying an electric voltage to the specimen. All electric field-assisted experiments were carried out in the same way: the dilatometer was set to increase the temperature from room temperature to 1100 or 1200 °C without any dwelling time, and to decrease the temperature to 200 °C. Heating and cooling rates were fixed to 10 °C min^{-1}. When the temperature of the dilatometer furnace reached 1100 or 1200 °C, an ac (1 kHz) electric voltage (usually corresponding to 100 V cm^{-1}) was applied to the specimen during 5 min. The electric current was limited to 5 A, a value we found to produce shrinkage in tin dioxide green pellets without visible deterioration.[3] The power surge was handled manually, the electric voltage as well as the maximum electric current being kept constant at each pulse. There was no automatic switching to electric current control as reported by other investigators.[21–23]

The sample was not allowed to cool down to the furnace temperature before the application of the next pulses in an attempt to force the shrinkage to the desired level or to the desired pulsing time (5 min, for example). The shrinkage level was monitored in the dilatometer and the voltage-current versus time data were collected in a data logger consisting of two (one for voltage and another for current) Fluke 8050A digital multimeters connected to a pc with a designed interface. The impedance spectroscopy analysis was carried out with a Hewlett Packard 4192A impedance analyzer in the 5–1.3 × 10^7 Hz frequency range in sintered specimens (with the parallel surfaces silver coated) positioned in a homemade sample chamber, which was

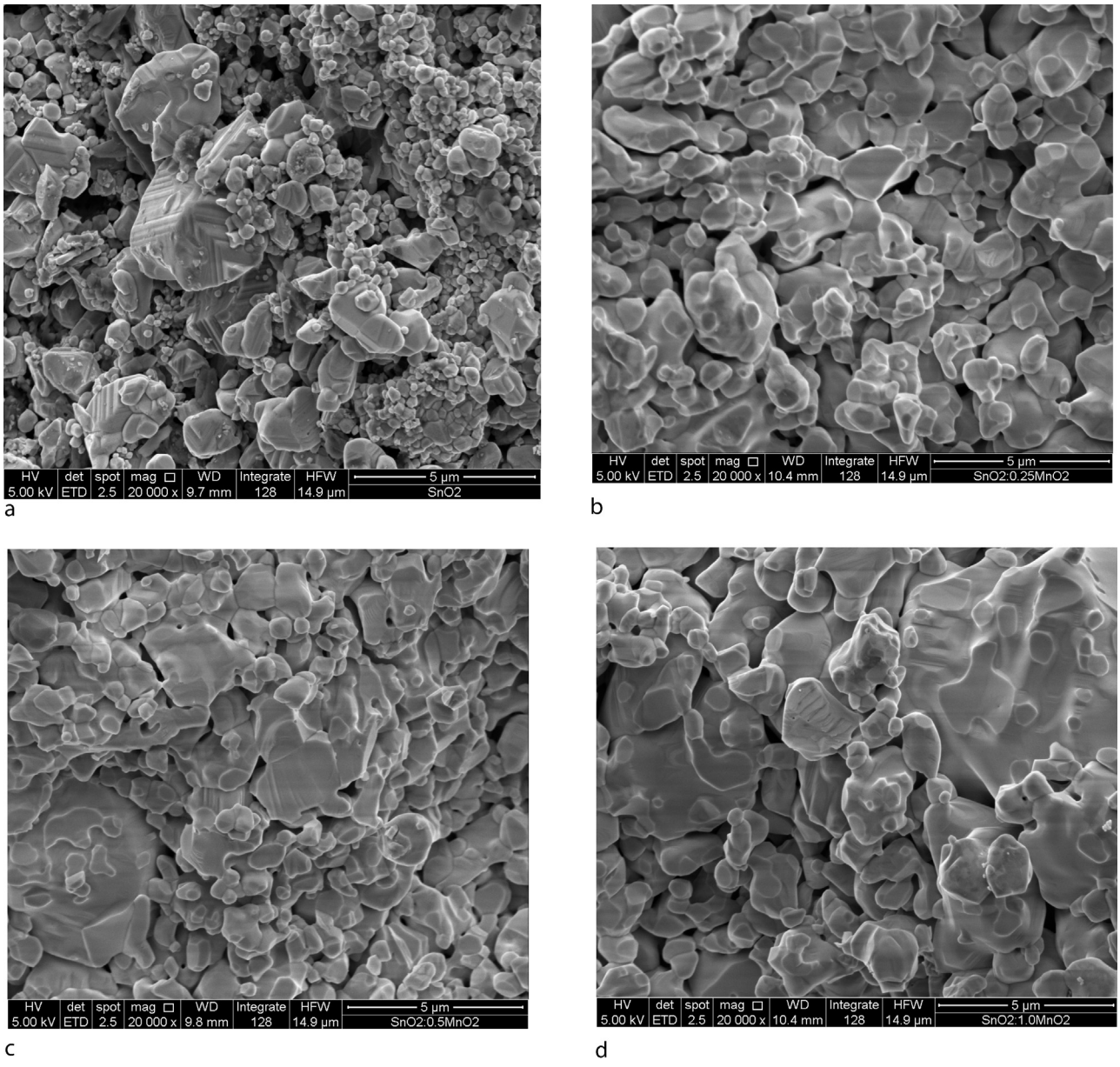

Fig. 2. Scanning electron microscopy micrographs of SnO_2:x% MnO_2, $x = 0$ (a), $x = 0.25$ (b), $x = 0.5$ (c), and $x = 1.0$ (d).

inserted in a programmable tubular furnace. After the electrical measurements, the samples were fractured for observation in a scanning electron microscope (Field Emission Gun FEI Inspect F50) operating at 5 kV, spot size 2.5.

3. Results and discussion

3.1. Effect of MnO_2 content

Fig. 1 shows the shrinkage behavior from room temperature to 1100 °C of SnO_2 green pellets prepared without and with mixing different amounts of MnO_2, with the continuous application of an ac voltage of 100 V cm^{-1}, 1 kHz, for 5 min after reaching 1100 °C, limiting the ac current to 5 A. All green pellets had similar diameter (5 mm) and thickness (5.3 mm). The application of the electric voltage promotes electric current pulses, each one leading to corresponding thickness variation, monitored in the dilatometer. The reason for limiting the electric current to 5 A is that higher currents were found to deliver enough heat to produce face to face open holes in the samples.

Apparently there are two shrinkage behaviors, most certainly related to two different sintering mechanisms: one due to the addition of manganese dioxide, which acts as sintering aid by creating oxygen vacancies on a shell region of the tin dioxide particles and consequently enabling inter-particle mass diffusion[7]; another due to the application of the electric field that acts as a promoter of Joule heating inside the specimen by the passage of the electric current through the specimen. In the former, the initial densification rate depends on the MnO_2 content added to SnO_2.[7] In the latter, the Joule heating delivered to the specimen weld together the neighboring particles.[3] A fair linear fitting is found for the shrinkage after the electric current pulses at

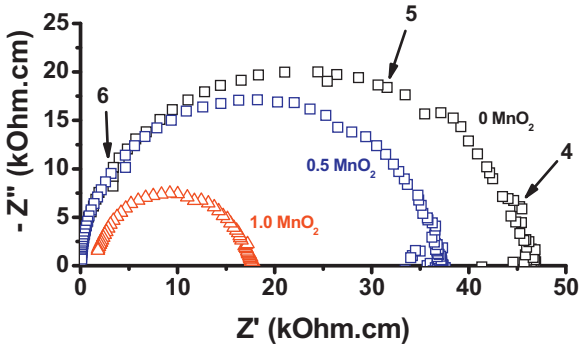

Fig. 3. Impedance plots of SnO_2:x wt.% MnO_2 (x = 0, 0.5 and 1.0) electric field-assisted sintered under the same conditions. Data collected at 540 °C. Numbers at arrows are log f (f:Hz).

1100 °C as a function of the manganese dioxide content added to the tin dioxide specimens (inset of Fig. 1a – manganese dioxide content/% shrinkage level: 0/9.94, 0.25/10.5, 0.5/11.4, 1.0/12.5). This means that using our experimental facility we are able to separate the contributions to shrinkage due to both mechanisms. It has been proposed, based on calculations of the power delivered to the specimen under dc bias, that the increase in temperature due to Joule heating is not sufficient to justify the extent of the electric field-assisted sintering in zirconia-based ceramics; a new mechanism has been proposed, taking into account the nucleation of point defects (Frenkel pairs) which could enhance mass transport and consequently sintering by intergranular diffusion.[24] Similar reasoning might be applied here, suggesting the creation of Schottky (and not Frenkel) pairs in tin dioxide.[25] In the same way oxygen vacancies created by manganese oxide doping enhances diffusion, nucleation of avalanche of oxygen vacancies would be produced by the electric current and promote sintering. In short, these shrinkages (Fig. 1a) would be caused by (i) Joule heating delivered by the electric current pulses, (ii) interparticle (mass) defect diffusion due to oxide ion vacancies created by manganese ion solution in the tin dioxide lattice and (iii) by oxide ion vacancies created by the electric field.

Another feature could be extracted from Fig. 1. Zooming the data between room temperature and 1100 °C, the onset temperature for shrinking (the departure from the straight lines drawn from RT to approximately 850 °C) have been evaluated, Fig. 1b. Fig. 1c shows the apparent linear relation between the onset temperature and the manganese dioxide content.

Fig. 2 shows the scanning electron microscopy micrographs of the electric field-assisted sintered samples depicted in Fig. 1.

The special feature in those micrographs (Figs. 2b–d) is the increase of grain growth with increasing MnO_2 content. The specimen without MnO_2 addition (Fig. 2a) contains relatively few well-developed grains with neighboring particles, which clearly have not lost their identity, i.e., were not affected by the electric current pulses. This might be an indication that the defects created by the reaction of MnO_2 with the surface of the SnO_2 do act as charge carriers for the action of the electric field upon sintering.

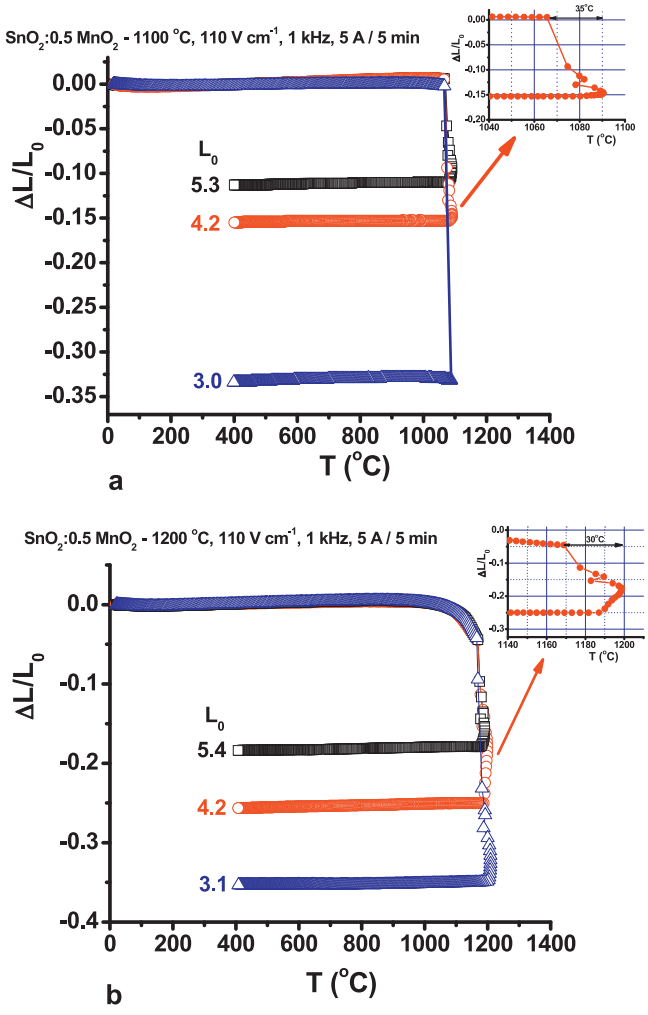

Fig. 4. Dilatometric curves of SnO_2:0.5 wt.% MnO_2 green compacts of different thickness upon electric field assisted sintering at near 1100 °C (a) and 1200 °C (b). Electric field 110 V cm^{-1} 5 min^{-1}, 1 kHz.

Fig. 3 shows impedance diagrams, measured at the same temperature, of SnO_2:MnO_2 electric field-assisted sintered specimens with different MnO_2 addition. The impedance diagrams consist of only one semicircle, typical of a non-metallic material inserted between the electrodes of a capacitor. The total electrical resistivity, evaluated at the intersection of the semicircle with the Z' axis at the low frequency limit, decreases for increasing manganese dioxide content. As the electrical resistivity reflects the contribution from the bulk and the interfaces (mainly pores), one may speculate that the average pore volume decreases for increasing MnO_2, known to be an efficient sintering aid.

3.2. *Effect of the thickness-to-diameter ratio*

Another important parameter to be considered during an electric field-assisted sintering experiment is the homogeneity in the distribution of the electric field in the specimen. This would assure an even distribution of the electric current lines and consequently an equal delivering of Joule heating throughout the whole specimen. In a polarized dielectric with cylindrical

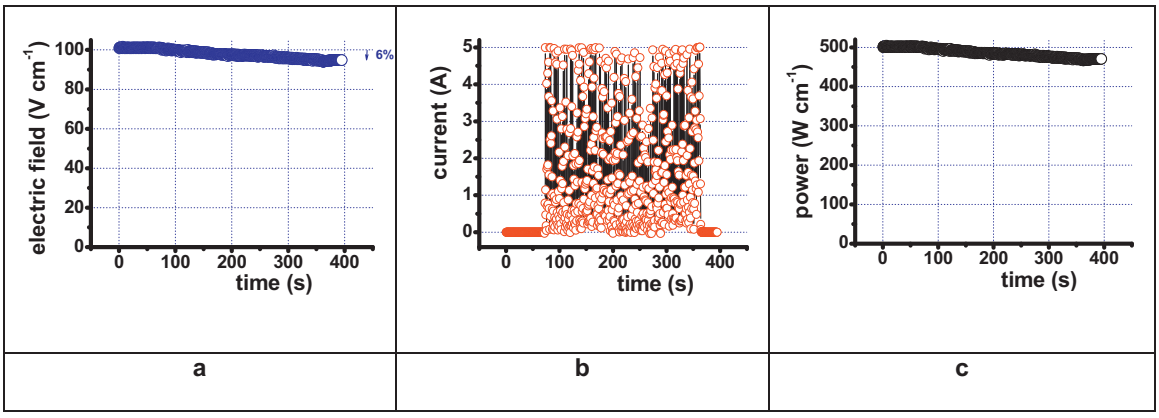

Fig. 5. Electric field-assisted sintering parameters on tin dioxide: electric field (a), electric current pulses (b) and electric power. Total pulse time: 5 min.

shape, the distribution of the electric current lines depends on the thickness-to-diameter ratio.

Fig. 4 shows the linear shrinkage, upon the same applied electric field setting the dilatometer temperature to 1100 °C (Fig. 4a) and to 1200 °C (4b), of similar (same distribution of particle size and same uniaxial and isostatic loads) cold pressed SnO_2:0.5 wt.% MnO_2 pellets with the same diameter but with different thickness. One should here point out the actual sample temperature is lower than the furnace temperature. The larger is the thickness the lower is the attained linear shrinkage upon electric current pulses. For thicknesses 5.3, 4.2 and 3.0 mm the measured shrinkage levels at 1100 °C were 11.3%, 15.6% and 33.4%, respectively. At 1200 °C those values were higher: 18.4%, 25.8% and 35.3%, as expected due to the higher mobility or diffusion coefficient of the chemical species responsible for the sintering process. Even though the applied field is the

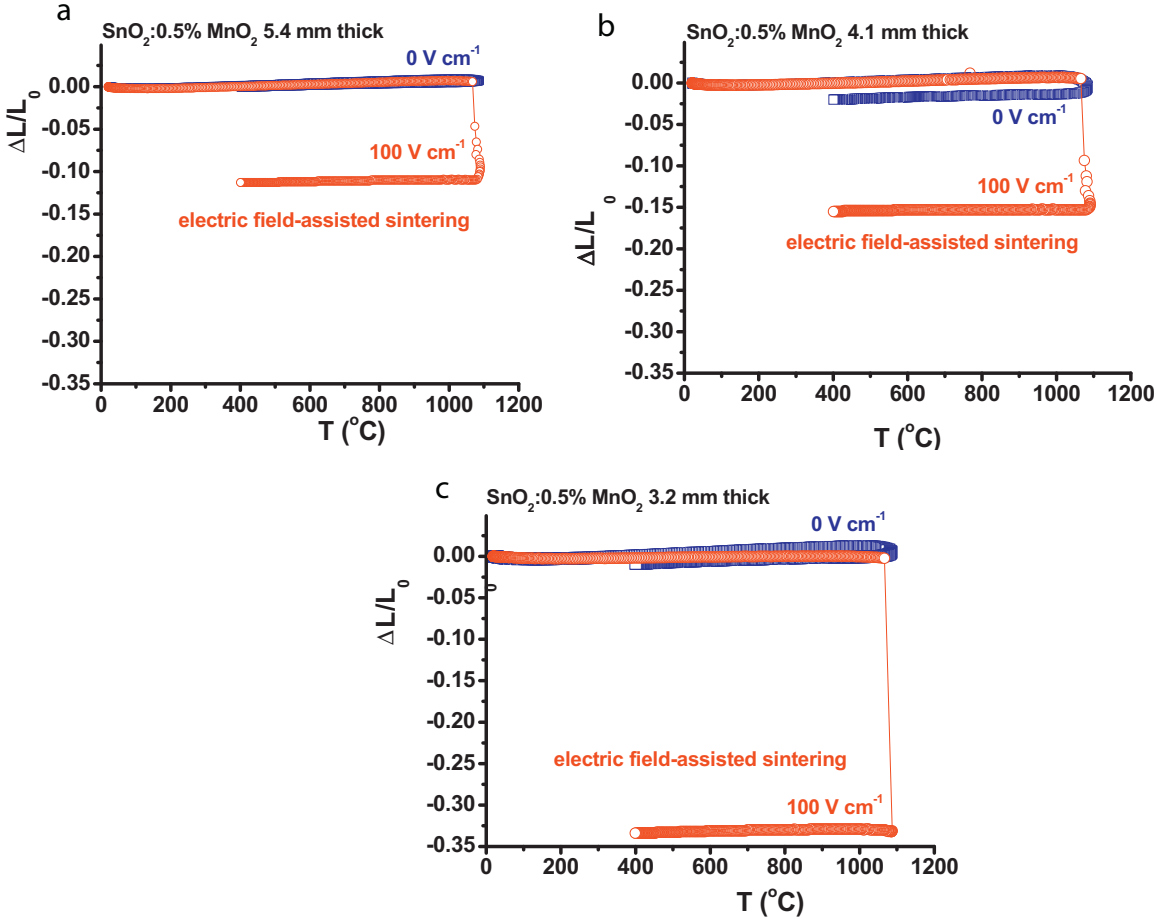

Fig. 6. Dilatometric curves of SnO_2:0.5 wt.% MnO_2 green compacts of different thickness without and with application of 110 V cm^{-1}, 1 kHz, near 1100 °C. (a) ~5 mm, (b) ~4 mm, (c) ~3 mm.

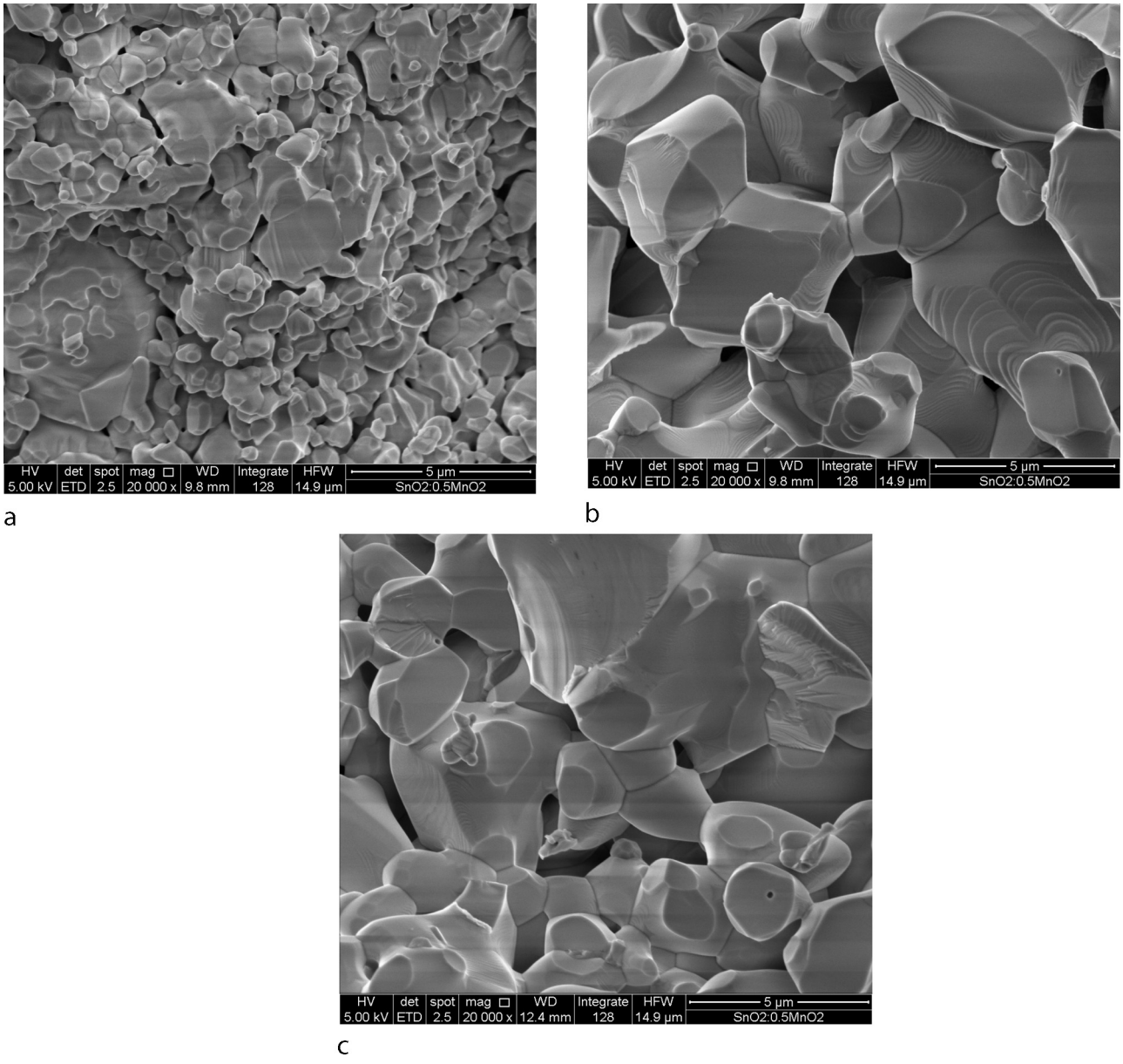

Fig. 7. FEG-SEM micrographs of SnO_2:0.5 wt.% MnO_2, electric field-assisted sintered at 1100 °C with 110 V cm^{-1}, 1000 Hz, 5 A limiting current. Thickness of the specimen before electric field-assisted sintering: (a) ~5 mm, (b) ~4 mm, (c) ~3 mm.

same, the thicker is the specimen the lower is the shrinkage. The power delivered to the specimens is the same but their volume is different and consequently the larger is the volume the lower is the Joule heating delivered to the sample. Moreover, the microstructure of specimens having different volumes might be different, i.e., their packing density, specific pore volume and residual stress may differ, leading to non-similar distribution of the electric current lines. Further experimental work is required to confirm this assumption.

Another interesting feature of those results is the increase in the sample temperature during the application of the electric current pulses, shown in the insets of Fig. 4a and b. Even though the dilatometer furnace does not provide heat to overcome the maximum set temperature, the thermocouple located near the sample indicates an increase of the temperature (nearly 30°!). This is further evidence that the electric current pulses promote Joule heating and that the sample delivers heating to its neighborhood.

Another important consideration is on the actual temperature the sample reaches during the electric current pulse. A model was presented based on the Stefan–Boltzmann law for black body radiation for estimating the temperature the sample reaches under the electric current pulse in a dc electric field-assisted sintering experiment.[12,14,22,24] Using Eq. (2)[24] $T = [T_0{}^4 + W/(A\sigma)]^{1/4}$, for $T_0 = 1100\,^{\circ}\mathrm{C}$ (1373 K), $W = W_{ac} = 50\,V \times 5\,\mathrm{A} \times \sqrt{2}/2 = 176.8\,\mathrm{W}$, $A = 2 \times 10^{-5}\,\mathrm{m}^2$, and $\sigma = 5.67 \times 10^{-8}\,\mathrm{W\,m^{-2}\,K^{-4}}$, one reaches the value of ~3300 °C, enough to reduce the SnO_2 to SnO and even to metallic Sn. This model, if correct, could be an explanation for the occurrence of small metallic Sn dots detected by EDS analysis on fracture surface of electric field-assisted tin dioxide.[3]

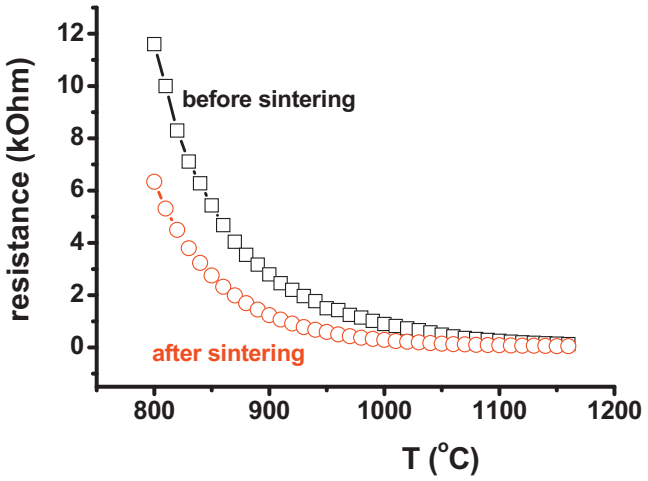

Fig. 8. Electrical resistance of SnO_2:0.5 mol% MnO_2 pellet (ϕ 5 mm × 4.2 mm) as a function of temperature before and after electric field-assisted sintering near 1200 °C. Heating and cooling rates: 10 °C min^{-1}.

Fig. 5 represents typical power dissipation during an electric field-assisted sintering of tin dioxide. Successive electric current pulses are delivered to the sample for 5 min under 100 V cm^{-1} stimuli. Only 6% degradation in the electric field is evaluated, probably because we do not allow the sample to reach the furnace temperature after each sequential flash.[26]

Fig. 6 shows the effect of the applied field to samples with different thicknesses. Each figure has two dilatometric curves: with and without application of the electric field, showing the enhanced shrinkage in the biased samples.

Fig. 7 shows the FEG-SEM micrographs of fracture surfaces of the SnO_2:0.5 wt.% MnO_2 after the electric field-assisted sintering procedure depicted in Fig. 4a.

A remarkable effect of the specimen thickness on the linear shrinkage is seen in those micrographs. Decreasing the specimen thickness produces a substantial increase of the average grain size. Experiments are underway to set the same shrinkage level to similar specimens with different thickness and to evaluate the average grain size. The thickness-to-diameter ratio seems to play an important role for designing appropriate methodology for electric field-assisted sintering ceramic pieces.

Fig. 8 shows a typical 2-probe electrical resistance data collected upon increasing the temperature before application of the electric voltage (before sintering) and during cooling down in the dilatometer (after sintering). The dependence of the electrical resistance on the temperature is similar, but after sintering the electrical resistance is lower due to pore elimination due to heating caused by the electric current pulses.

4. Conclusions

The larger is the amount of MnO_2 added to SnO_2, the higher is the shrinkage level reached upon electric field-assisted sintering. This means that the electric current pulses enhance the sintering rate due to vacancy diffusion. This enhancement may be attributed to the increase in the inter-particle temperature caused by the intense Joule heating delivered locally during the electric current pulses, simultaneously detected at the dilatometer thermocouple located close to the specimen. An additional mechanism, similar to the one proposed by Raj[24] for yttria stabilized zirconia, based on the formation of Schottky defects caused by the passage of the electric current through the tin dioxide specimen, is suggested to promote sintering by enhancing oxide ion vacancy diffusion. Another interesting feature is that the applied voltage per volume unit should be taken into account if ceramic pieces of different shape and size are to be sintered to the same shrinkage level.

Acknowledgements

To CNEN (Brazilian Nuclear Energy Commission) and CNPq (Brazilian NRC) for financial support.

References

1. Bueno PR, Varela JA, Longo E. SnO_2, ZnO and related polycrystalline compound semiconductors: an overview and review on the voltage-dependent resistance (non-ohmic) feature. *J Eur Ceram Soc* 2008;**28**:505–29.
2. Wang H, Rogash AL. Hierarchical SnO_2 nanostructures: recent advances in design, synthesis, and applications. *Chem Mater* 2014;**26**:123–33.
3. Muccillo R, Muccillo ENS. Electric field-assisted flash sintering of tin dioxide. *J Eur Ceram Soc* 2013;**34**:915–23.
4. Quadir T, Ready DW. Microstructure evolution in SnO_2 and CdO in reducing atmospheres. *Mater Sci Res* 1984;**16**:159–69.
5. Park SJ, Hirota K, Yamamura H. Densification of nonadditive SnO_2 by hot isostatic pressing. *Ceram Int* 1985;**11**:158.
6. Kimura T, Inada S, Yamaguchi T. Microstructure development in SnO_2 with and without additives. *J Mater Sci* 1989;**24**:220–6.
7. Gouvea D, Smith A, Bonnet JP, Varela JA. Densification and coarsening of SnO_2-based materials containing manganese oxide. *J Eur Ceram Soc* 1998;**18**:345–51.
8. Las WC, Gouvea D, Sano W. EPR of Mn as densifying agent in SnO_2 powders. *Solid State Sci* 1999;**1**:331–7.
9. Gouvea D, Smith A, Smith DS, Bonnet JP, Varela JA. Translucent tin dioxide ceramics obtained by natural sintering. *J Eur Ceram Soc* 1997;**80**:2735–6.
10. Zapata-Solvas E, Bonilla S, Wilson PR, Todd RI. Preliminary investigation of flash sintering of SiC. *J Eur Ceram Soc* 2013;**33**:2811–6.
11. Jha Sikkar K, Rishi Raj. The effect of electric field on sintering and electrical conductivity of titania. *J Am Ceram Soc* 2014;**97**:527–34.
12. Yang D, Raj R, Conrad H. Enhanced sintering rate of zirconia (3Y-TZP) through the effect of a weak dc electric field on grain growth. *J Am Ceram Soc* 2010;**93**:2935–7.
13. Ghosh S, Chokshi AH, Lee P, Raj R. A huge effect of weak dc electrical fields on grain growth in zirconia. *J Am Ceram Soc* 2009;**92**:1856–9.
14. Cologna M, Rashkova B, Raj R. Flash sintering of nanograin zirconia in <5 s at 850 °C. *J Am Ceram Soc* 2010;**93**:3556–9.
15. Cologna M, Prette ALG, Raj R. Flash-sintering of cubic yttria-stabilized zirconia at 750 °C for possible use in SOFC manufacturing. *J Am Ceram Soc* 2011;**94**:316–9.
16. Cologna M, Francis JSC, Raj R. Field assisted and flash sintering of alumina and its relationship to conductivity and MgO-doping. *J Eur Ceram Soc* 2011;**31**:2827–37.
17. Prette ALG, Cologna M, Sglavo VM, Raj R. Flash sintering of Co_2MnO_4 spinel for solid oxide fuel cell applications. *J Power Sources* 2011;**196**:2061–5.
18. Raj R, Cologna M, Francis JSC. Influence of externally imposed and internally generated electrical fields on grain growth, diffusional creep, sintering and related phenomena in ceramics. *J Am Ceram Soc* 2011;**94**:1941–65.

19. Brook RJ. Frontiers of sinterability. In: Handwerker CA, Blendell JE, Kaysser WA, editors. *Ceramic transactions – sintering of advanced ceramics*, vol. 7. The American Ceramic Society; 1990.
20. Muccillo R, Muccillo ENS. An experimental setup for shrinkage evaluation during electric field-assisted flash sintering: application to yttria-stabilized zirconia. *J Eur Ceram Soc* 2013;**33**:515–20.
21. Francis JSC, Cologna M, Raj R. Particle size effects in flash sintering. *J Eur Ceram Soc* 2012;**32**:3129–36.
22. Francis JSC, Raj R. Flash sintering of nanograin zirconia. *J Am Ceram Soc* 2012;**95**:138–46.
23. Naik KS, Sglavo VM, Raj R. Field assisted sintering of ceramic constituted by alumina and yttria stabilized zirconia. *J Eur Ceram Soc* 2014;**34**:2435–42.
24. Raj R. Joule heating during flash-sintering. *J Eur Ceram Soc* 2012;**32**:2293–301.
25. Godinho KG, Walsh A, Watson GW. Energetic and electronic structure analysis of intrinsic defects in SnO_2. *J Phys Chem C* 2009;**113**:439–48.
26. Francis JSC, Raj R. Influence of the field and the current limit on flash sintering at isothermal furnace temperatures. *J Am Ceram Soc* 2013;**96**:2754–8.